

Research Article

SNR and Discretization Enhancement for System Matrix Determination by Decreasing the Gradient in Magnetic Particle Imaging

Matthias Graeser* · Anselm von Gladiss · Thomas Friedrich · Thorsten M. Buzug

Institute of Medical Engineering, University of Lübeck, Lübeck, Germany

*Corresponding author, email: {graeser,buzug}@imt.uni-luebeck.de

Received 25 November 2016; Accepted 25 February 2017; Published online 23 March 2017

© 2017 Graeser; licensee Infinite Science Publishing GmbH

This is an Open Access article distributed under the terms of the Creative Commons Attribution License (<http://creativecommons.org/licenses/by/4.0>), which permits unrestricted use, distribution, and reproduction in any medium, provided the original work is properly cited.

Abstract

In system matrix (SM) based reconstruction, the physical resolution is often within the range of the SM discretization. This is caused by the signal to noise ratio (SNR) decrease following a discretization increase due to the smaller particle sample volume. As the SNR affects the resolution of the image as well, it is necessary to decouple the SNR and discretization. In this work, a calibration protocol is presented which enhances either the SNR or discretization by reducing the gradient strength within the system calibration. This new protocol results in higher resolution and better image quality.

I. Introduction

In Magnetic Particle Imaging (MPI), the image reconstruction can be performed either in time space (x-space reconstruction) or in frequency space (system matrix reconstruction) [1, 2]. However, for complex spatial encoding trajectories like Lissajous trajectories, the x-space reconstruction technique introduces some artifacts that are not visible in the system matrix (SM) reconstruction approach [3]. The SM technique itself has many drawbacks, including long calibration scans, a limit in discretization due to the signal to noise ratio (SNR), and the impact of the regularization which makes images hardly comparable.

The first two of these issues can be overcome by either using a system calibration unit (SCU), or a focus field approach to determine the SM [4–6]. This paper shows a different method to overcome the limit of SNR and discretization by adapting the gradient and FOV size to the sample volume. This enables to either increase the discretization or SNR cubically, limited only by the bore

size and field homogeneity. An advantage of this method is, that, as it uses the MPI scanner for SM determination, no transfer function is needed.

II. Methods

II.1. Theoretical Background

In SM based reconstruction, the system matrix is acquired prior to a measurement. For doing that, a particle sample is positioned subsequently at each spatial position of the field of view (FOV) within a defined grid. At each position, the imaging sequence is started and the system frequency response is stored as a column in the system matrix. After that, the system matrix can be used for image reconstruction [7, 8]. In some cases, the achievable resolution for a scanner might be below the discretization limited due to SNR reasons [5]. Due to the long calibration time of the SM approach, averaging is only feasible as long as the robot movement is the limiting time factor. For these cases a method to increase

Table 1: SM calibration parameters. To investigate SNR increase and discretization increase as well as a combination of both, three gradient values are measured.

Sample edge length / mm	1	1	2	2
Gradient strength / Tm ⁻¹	2.5	1.25	1.25	0.625
Drive Field FOV / mm	19.2 × 9.6	38.4 × 19.2	38.4 × 19.2	76.8 × 38.4
SM FOV / mm	22 × 12	44 × 24	44 × 24	88 × 48
FOV Grid	22 × 12	44 × 24	22 × 12	44 × 24

the discretization without the need of more averaging for the SM determination is needed. For most field free point (FFP) scanners the drive field strength is assumed to be homogeneous within the FOV. The SM dependency is then reduced to the selection field. The field strength can be described as

$$\mathbf{H}_{\text{SF}}(r) = \mathbf{G} \circ \mathbf{r}, \quad (1)$$

with \circ being the point-wise multiplication operator. Assuming the gradient to be spatially independent a simple scaling can be derived:

$$\frac{\mathbf{G}}{\alpha} \circ \alpha \mathbf{r} = \mathbf{G} \circ \mathbf{r}, \quad (2)$$

with α being the scaling factor. For a real world scanner the assumption of a constant gradient strength is only valid within a limited region, also limiting the range of this method. A nonlinear gradient would introduce deformations in the resulting image. This dependency is exploited to increase the SNR and discretization of the SM.

II.II. Increase in Discretization

To investigate the scaling of the SM, its the determination is done with different gradients and sample sizes. The gradient is reduced from a maximum of 2.5 T/m in three steps to a limit of $2.5/4 \text{ T/m} = 0.625 \text{ T/m}$. As the drive field strength \mathbf{H}_{DF} is kept constant, the FOV is increased due to

$$FOV_{\text{border}} \in [\mathbf{H}_{\text{DF}} \oslash \mathbf{G}], \quad (3)$$

with \oslash being the point-wise division operator. The step size is hold constant and using the same particle - sample size, which leads to a corresponding increase calibration points.

II.III. Increase of SNR

If the discretization is sufficient, the same technique can be used to enhance the SNR. Therefore the step size is doubled to cope for the higher FOV and inserting a bigger sample volume. As the SNR scales directly with the absolute iron concentration in the sample, the increase in SNR is approximately proportional to the voxel volume.

For a quantitative image the system matrix has to be divided by the volume ratio of the voxel sizes. Otherwise images reconstructed with bigger calibration samples will result in an underestimated concentration.

II.IV. Experiments

SM Measurements

To investigate the described technique experiments are done with the Bruker Preclinical MPI Scanner situated at the University of Lübeck. The coordinate system within the scanner is defined as the bore direction being x, left/right direction being y and up/down being z. The strong gradient direction is situated parallel to the z direction. Without loss of generality all measurements were taken using a 2D excitation within the xz-plane of the scanner. We investigate three different gradient strengths at 2.5 T/m, 1.25 T/m and 0.625 T/m were investigated, respectively. SM measurements were performed with a $1 \times 1 \times 1 \text{ mm}^3$ cubic sample for the 2.5 T/m and 1.25 T/m gradient strengths and with a $2 \times 2 \times 2 \text{ mm}^3$ cubic sample for the 1.25 T/m, 0.625 T/m gradients. The used tracer for SM measurements were undiluted Resovist. All SM measurements were taken with 12 mT drive-field strength in both directions and are averaged 10 times. The corresponding grids and measurement times are shown in Tab. 1.

Phantom Measurements

To investigate the possibility of image reconstruction a resolution phantom is designed. This phantom consists of three glass capillaries with 0.5 mm inner diameter that can be placed within a grid of 1 mm on the z axis and 1.5 mm on the x axis. The capillaries are filled with 1:3 diluted Resovist (0.125 mmol/ml). The wall thickness of the capillaries is 0.25 mm, which can be arranged in distances by multiples of 1 mm plus 0.5 mm wall thickness for z direction and multiples of 1.5 mm plus 0.5 mm wall thickness for x direction. The measurement is taken with 2.5 T/m gradient and 12 mT drive- field magnitude. As the effect of the SM SNR is to be studied in this work, the phantom measurements are averaged 100 times to provide a higher SNR than the SMs. The phantoms used is shown in Fig. 1.

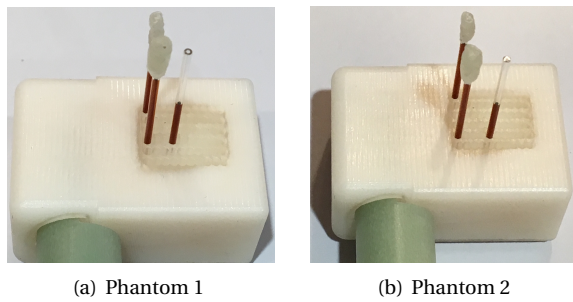


Figure 1: Imaging phantom used for the experiments. The phantom consists of a grid for placing glass capillaries. The step size is 1 mm in z direction and 1.5 mm in x direction.

III. Results

III.I. System Matrices

Fig. 2 shows selected SM components for all four SM sets. As expected, the SM taken with the 2 mm sample size shows an overall better SNR as it provides $2^3 = 8$ times the amount of nanoparticles. In Fig. 3, the SNR of all SMs are plotted for all frequency components used in this work. The advantage of the bigger sample is visible as it provides higher SNR and allows more frequencies for reconstruction than the smaller samples. Reducing the gradient to 0.625 T/m leads to an increase in the variance of the background signal, which results in a smaller SNR compared to the 1.25 T/m gradient. This is especially visible in the higher frequency components where no patterns can be visualized for, the strong gradient.

III.II. Image Reconstruction

Fig. 4 and Fig. 5 show the reconstruction results of the phantom measurements using a Kaczmarz algorithm. In Fig. 4 the reconstruction parameters is optimized for the smaller calibration samples. The three dots can be separated for all SMs in case of the second phantom. For the first phantom only the dots aligned in the strong gradient direction can be separated. Due to the high SNR of the bigger calibration sample a higher number of iterations can be chosen for the 8 μ l SMs. This lead to a much lower blurring of the dots and sharper images, so that the dots of the first phantom can be separated. The best result is achieved for the 2 mm SM with 0.625 T/m gradient. The reconstruction parameters were kept constant for each figure.

IV. Conclusion and Discussion

It was shown, that the SNR and discretization enhancement is possible by decreasing the gradient together with either increasing the discretization or with increasing the

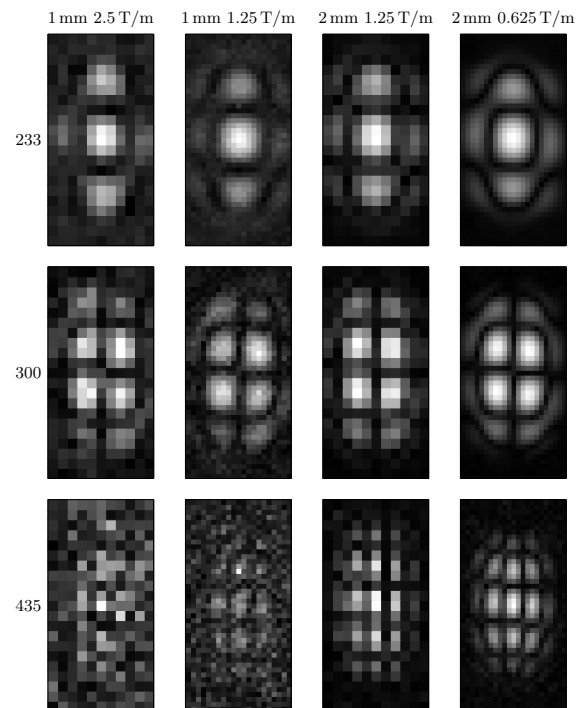


Figure 2: Selected SM components of the x channel for the four different SM. Even with the lowest gradient, no distortion due to inhomogeneities can be seen.

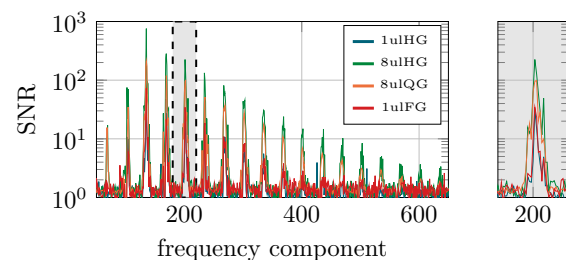


Figure 3: SNR of the x-channel. It can be seen that the SNR of the bigger calibration samples is approximately 8 times higher. However, while the two 1 μ l samples show nearly the same SNR, the two 8 μ l samples differ. This is caused by a larger variance of the background signal which is expected for low gradient strength.

sample volume. The results show not only an artifact-free image but also an increased resolution due to the better SNR of the SM and the higher discretization. In this work, the method has been investigated with respect to the xz plane. Following the same protocol, the FOV would be closer to the bore limit if the y direction is included. This might result in inhomogeneities which would distort the SM for low gradients and therefore introduce artifacts in the reconstruction. If the field profile is well known, this might also be addressed by a non equidistant grid. Instead, a constant field step may be introduced. However, inhomogeneities caused by the drive field coils can

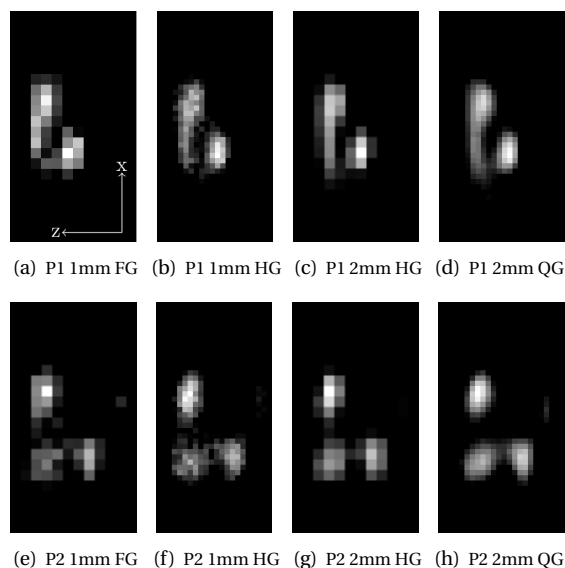


Figure 4: Imaging results of two phantoms consisting of three glass capillaries filled with 1:3 diluted Resovist. The image caption stands for phantom 1 and 2 (P1, P2) full, half and quarter gradient (FG,HG, QG). The dot distance for P1 is 2.5 mm on the z axis and 3.5 mm on the x axis. For P2 the distance is 3.5 mm in z direction and is 3.5 mm in xz direction. The reconstruction parameter were optimized for low SNR system matrices. Reconstruction parameters: SNR threshold: 4, iterations=10, $\lambda=1e-6$, included frequency components: 66.

hardly be corrected as this directly influences the signal generation of the particles. This method can still be used to enhance the discretization in the center of the FOV. In many cases one is especially interested in objects lying in the center of an image and therefore, one might introduce different voxel sizes for the middle part of the FOV and the outer part of the FOV. Such non equidistant grids can enhance the resolution in the center of the image. A further decrease of the gradient to lower values as shown here seems not suitable for the used scanner geometry. Due to the scanner bore of 11.8 mm diameter the further decrease will lead the FFP outside the bore.

Acknowledgements

We thankfully acknowledge the financial support of the German Research Foundation (DFG) and the Federal Ministry of Education and Research (BMBF) (Grant Numbers BU 1436/10-1 and 13GW0069A).

References

- [1] B. Gleich and J. Weizenecker. Tomographic imaging using the nonlinear response of magnetic particles. *Nature*, 435(7046):1214–1217, 2005. doi:[10.1038/nature03808](https://doi.org/10.1038/nature03808).

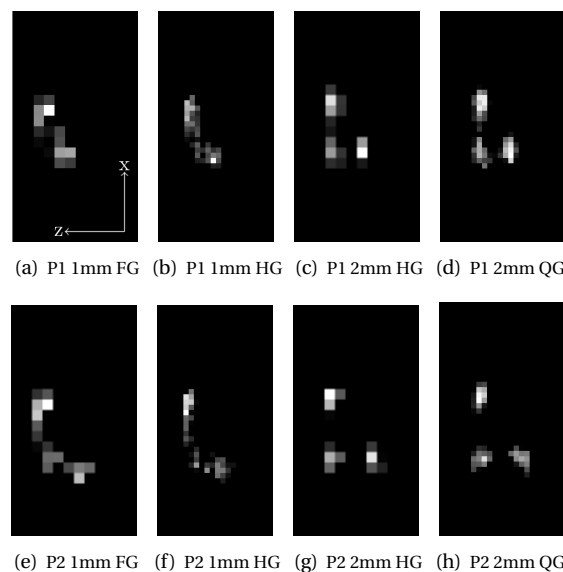


Figure 5: Imaging results of two phantoms consisting of three glass capillaries filled with 1:3 diluted Resovist. The image caption stands for phantom 1 and 2 (P1, P2) full, half and quarter gradient (FG,HG, QG). The dot distance for P1 is 2.5 mm for the z axis and 3.5 mm on the x axis. For P2 the distance is 3.5 mm in z direction and is 3.5 mm in xz direction. The reconstruction parameter were optimized for low SNR system matrices. Reconstruction parameters: SNR threshold: 4, iterations=300, $\lambda=5e-5$, included frequency components: 66.

- [2] P. W. Goodwill and S. M. Conolly. The x-Space Formulation of the Magnetic Particle Imaging process: One-Dimensional Signal, Resolution, Bandwidth, SNR, SAR, and Magnetostimulation. *IEEE Trans. Med. Imag.*, 29(11):1851–1859, 2010. doi:[10.1109/TMI.2010.2052284](https://doi.org/10.1109/TMI.2010.2052284).
- [3] A. Cordes, C. Kaethner, M. Ahlberg, and T. M. Buzug. X-space Deconvolution for Multidimensional Lissajous-based Data-Acquisition Schemes. In *International Workshop on Magnetic Particle Imaging (IWMPI) 2016, Book of Abstracts*, page 74, 2016.
- [4] M. Graeser, A. von Gladiss, M. Weber, and T. M. Buzug. Two dimensional magnetic particle spectrometry. *Phys. Med. Biol.*, [accepted for publication], 2017. doi:[10.1088/1361-6560/aa5bcd](https://doi.org/10.1088/1361-6560/aa5bcd).
- [5] A. von Gladiss, M. Graeser, P. Szwargulski, T. Knopp, and T. M. Buzug. Hybrid system calibration for multidimensional magnetic particle imaging. *Phys. Med. Biol.*, [accepted for publication], 2017. doi:[10.1088/1361-6560/aa5340](https://doi.org/10.1088/1361-6560/aa5340).
- [6] A. Halkola, T. M. Buzug, J. Rahmer, B. Gleich, and C. Bontus. System Calibration Unit for Magnetic Particle Imaging: Focus Field Based System Function. In *Springer Proceedings in Physics*, volume 140, pages 27–31. Springer, Berlin/Heidelberg, 2012. doi:[10.1007/978-3-642-24133-8_5](https://doi.org/10.1007/978-3-642-24133-8_5).
- [7] M. Grüttner, T. Knopp, J. Franke, M. Heidenreich, J. Rahmer, A. Halkola, C. Kaethner, J. Borgert, and T. M. Buzug. On the formulation of the image reconstruction problem in magnetic particle imaging. *Biomed. Tech. / Biomed. Eng.*, 58(6):583–591, 2013. doi:[10.1515/bmt-2012-0063](https://doi.org/10.1515/bmt-2012-0063).
- [8] J. Rahmer, J. Weizenecker, B. Gleich, and J. Borgert. Analysis of a 3-D System Function Measured for Magnetic Particle Imaging. *IEEE Trans. Med. Imag.*, 31(6):1289–1299, 2012. doi:[10.1109/TMI.2012.2188639](https://doi.org/10.1109/TMI.2012.2188639).